Experimental realization of $1 \rightarrow 2$ asymmetric phase-covariant quantum cloning

Hongwei Chen,[1] Xianyi Zhou,[1] Dieter Suter,[2] and Jiangfeng Du[1,2,*]

[1]*Hefei National Laboratory for Physical Sciences at Microscale and Department of Modern Physics, University of Science and Technology of China, Hefei, Anhui 230026, People's Republic of China*

[2]*Fachbereich Physik, Universität Dortmund, 44221 Dortmund, Germany*

(Received 29 November 2006; revised manuscript received 21 December 2006; published 17 January 2007)

While exact cloning of an unknown quantum state is prohibited by the linearity of quantum mechanics, approximate cloning is possible and has been used, e.g., to derive limits on the security of quantum communication protocols. In the case of asymmetric cloning, the information from the input state is distributed asymmetrically between the different output states. Here, we consider asymmetric phase-covariant cloning, where the goal is to optimally transfer the phase information from a single input qubit to different output qubits. We construct an optimal quantum cloning machine for two qubits that does not require ancilla qubits and implement it on an NMR quantum information processor.

DOI: 10.1103/PhysRevA.75.012317 PACS number(s): 03.67.Dd, 76.60.−k

I. INTRODUCTION

Among the main differences between quantum and classical information is the fundamental impossibility to exactly duplicate an unknown quantum state. This was established by the no-cloning theorem of Dieks [1] and Wootters and Zurek [2]; for a review, see Ref. [3]. While *exact* cloning is thus impossible, it remains an important goal to *approximately* clone quantum states. This possibility, which is particularly important for quantum communication and cryptography, was first discussed by Bužek and Hillery [4], who showed that it is possible to create copies (approximate clones) of unknown quantum states with a quality that does not depend on the initial state.

Approximate cloning can be optimized in different ways. In so-called asymmetric cloning, the amount of information transferred from the input state to the copy is an adjustable parameter. The quality of the copy and the distortion that the cloning process causes on the original system both depend on this parameter: If the quality of the copy increases, the distortion of the original necessarily increases simultaneously [5–8]. This is quantified by the fidelity of the two output systems, which is defined as the overlap of these states with the input state. This tradeoff relates, e.g., the amount of information that an eavesdropper can extract from a quantum communication channel to the error rate of the transmitted information [9].

Asymmetric quantum cloning was first proposed for copying a single qubit to a single-copy qubit [6], and subsequently extended to arbitrary dimensions (including the continuous case) [10,11]. An implementation of universal asymmetric cloning in an optical experiment was proposed locally [12] and at a distance [13]. An experimental realization of $1 \rightarrow 2$ asymmetric cloning was reported by Zhao *et al.* [14] using two entangled photon pairs.

The quality of the cloning can be improved if the initial state is restricted to part of the full Hilbert space. An example of this state-dependent cloning is phase-covariant cloning [15], where the input state is an equal-weight superposition of two basis states. The goal is then to optimally clone the state in such a way that the phase information is conserved.

In this paper, we construct a two-qubit quantum logic circuit that implements the optimal asymmetric $1 \rightarrow 2$ phase-covariant cloning [15] for arbitrary input phase. Our cloning machine does not require any ancilla qubits and uses only two gate operations. The cloning process is implemented experimentally in an NMR system, using nuclear-spin qubits. For the gate operations we use controlled geometrical phase gates and demonstrate the trade-off in fidelity for the two output qubits.

II. CLONING SCHEME

In the following, we consider phase-covariant cloning: the original qubit to be cloned is in an equal-weight superposition of the two basis states,

$$|\psi\rangle_{ini} = \frac{1}{\sqrt{2}}(|0\rangle + e^{i\varphi}|1\rangle), \tag{1}$$

with an unknown phase difference φ. We clone this state onto a second qubit that is originally in state $|0\rangle$. The cloning is accomplished by a unitary operation acting on the initial product state $|\psi\rangle_{ini}|0\rangle$ [16]. The operation can be specified by its effect on the two orthogonal initial states $|00\rangle$ and $|10\rangle$,

$$|00\rangle \rightarrow |00\rangle,$$

$$|10\rangle \rightarrow \cos\frac{\alpha}{2}|10\rangle + \sin\frac{\alpha}{2}|01\rangle, \tag{2}$$

or by its matrix representation

$$u_n = \begin{pmatrix} 1 & 0 & 0 & 0 \\ 0 & 0 & \sin\left(\frac{\alpha}{2}\right) & \cos\left(\frac{\alpha}{2}\right) \\ 0 & 0 & \cos\left(\frac{\alpha}{2}\right) & -\sin\left(\frac{\alpha}{2}\right) \\ 0 & -1 & 0 & 0 \end{pmatrix}. \tag{3}$$

This operation is equivalent (up to local operation and

*Electronic address: djf@ustc.edu.cn

phases) to $\mathrm{CROT}_{12}\mathrm{CNOT}_{21}$ (CROT denotes controlled rotation gate and CNOT denotes controlled-NOT gate), and the rotation angle α can be used to adjust how much information is transferred to the second qubit.

After the cloning operation, the partial density operators for the two qubits are

$$\rho_a = \frac{1}{2}\begin{pmatrix} 1+\sin^2\frac{\alpha}{2} & e^{-i\varphi}\cos\frac{\alpha}{2} \\ e^{i\varphi}\cos\frac{\alpha}{2} & 1-\sin^2\frac{\alpha}{2} \end{pmatrix},$$

$$\rho_b = \frac{1}{2}\begin{pmatrix} 1+\cos^2\frac{\alpha}{2} & e^{-i\varphi}\sin\frac{\alpha}{2} \\ e^{i\varphi}\sin\frac{\alpha}{2} & 1-\cos^2\frac{\alpha}{2} \end{pmatrix}. \quad (4)$$

The state overlap between the original and the two output qubits are

$$F_a = \mathrm{Tr}(\rho_a|\psi\rangle_{ini}\langle\psi|_{ini}) = \frac{1+\cos\frac{\alpha}{2}}{2},$$

$$F_b = \mathrm{Tr}(\rho_b|\psi\rangle_{ini}\langle\psi|_{ini}) = \frac{1+\sin\frac{\alpha}{2}}{2}. \quad (5)$$

The choice of the angle α thus determines how much information is transferred from qubit a to qubit b: For $\alpha=0$, the overlap of qubit a with the initial state is 1, while the overlap of the copy qubit is just the random value $\frac{1}{2}$. When $\alpha=\frac{\pi}{2}$, we obtain the case of optical symmetric cloning, with $F_a=F_b \simeq 0.85355$, which has been shown to be the optimal value for symmetric phase-covariant cloning [15]. For $\alpha=\pi$, the information is transferred completely to the copy qubit, with $F_a=\frac{1}{2}, F_b=1$.

Compared to the logic circuit of the symmetric cloning machine proposed in Ref. [17], this scheme needs fewer logic gates. We therefore expect it to perform better in practice, being less affected by experimental imperfections, such as errors in rotation angles of radio-frequency pulses.

III. GEOMETRIC PHASE GATE

Geometric quantum phases [20–23] have the remarkable property that they depend only on global parameters (e.g., the area of a circuit) and are therefore not sensitive to some local variations of the trajectory. It was therefore suggested that quantum gate operations using geometric gates may be less susceptible to experimental imperfections and therefore yield higher fidelity [19,24–33].

We therefore used geometric phase gates to implement the two controlled-gate operations required for the cloning operation (3) (see Fig. 1). We first discuss the relevant operation for a single qubit and then extend the procedure to the controlled operations.

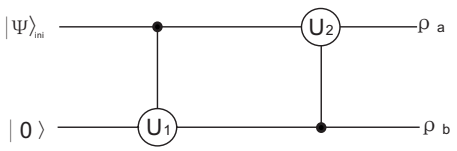

FIG. 1. Quantum logic circuit for our optimal asymmetric quantum phase-covariant cloning machine. Qubit a is the one to be cloned, initially in the state $|\psi\rangle_{ini}$, while qubit b is the blank one, which is initially in state $|0\rangle$. The unitary operation U_1 denotes $R_y(\alpha)$ and U_2 denotes $R_y(-\pi)$.

A. Single-qubit gate

Within the two-level system, we consider two orthogonal states $|\psi_+\rangle$ and $|\psi_-\rangle$, which undergo a cyclic evolution described by the operator $U(\tau)$: $U(\tau)|\psi_\pm\rangle = e^{\pm i\gamma}|\psi_\pm\rangle$. The parameter γ is thus the total phase difference of the two states acquired during this circuit.

In the computational basis ($|0\rangle$, $|1\rangle$), the cyclic states can be written as

$$|\psi_+\rangle = \cos\frac{\chi}{2}|0\rangle + e^{i\varphi}\sin\frac{\chi}{2}|1\rangle,$$

$$|\psi_-\rangle = \sin\frac{\chi}{2}|0\rangle - e^{i\varphi}\cos\frac{\chi}{2}|1\rangle,$$

where (χ,φ) are the spherical coordinates of the state vector on the Bloch sphere. For an arbitrary input state $|\psi_{in}\rangle = a_+|\psi_+\rangle + a_-|\psi_-\rangle$ with $a_\pm = \langle\psi_\pm|\psi_{in}\rangle$, after the cyclic evolution for the $|\psi_\pm\rangle$ state, the output state is $|\psi_{out}\rangle = U(\gamma,\chi,\varphi)|\psi_{in}\rangle$, where

$$U = \begin{pmatrix} e^{i\gamma}\cos^2\frac{\chi}{2} + e^{-i\gamma}\sin^2\frac{\chi}{2} & ie^{-i\varphi}\sin\gamma\sin\chi \\ ie^{i\varphi}\sin\gamma\sin\chi & e^{i\gamma}\sin^2\frac{\chi}{2} + e^{-i\gamma}\cos^2\frac{\chi}{2} \end{pmatrix}. \quad (6)$$

This operation becomes a purely geometric gate operation if the dynamic contribution to the total phase γ vanishes.

In the experiment, we use a nonadiabatic geometric phase and transform the input states along geodesic circuits on the Bloch sphere, as shown in Fig. 2. Here, the cyclic states are

$$|\psi_+\rangle = \frac{1}{\sqrt{2}}(|0\rangle + i|1\rangle), \quad |\psi_-\rangle = \frac{1}{\sqrt{2}}(|0\rangle - i|1\rangle),$$

i.e., $\chi=\varphi=\frac{\pi}{2}$. For the circuit shown in Fig. 2, the solid angle subtended by the circuit is equal to α, the rotation angle during the second part of the circuit. The geometric phase becomes thus $\gamma=-\frac{\alpha}{2}$.

For the circuit of Fig. 2, we may substitute the above values for χ, φ, and γ. The propagator becomes then

$$U\left(-\frac{\alpha}{2},\frac{\pi}{2},\frac{\pi}{2}\right) = \begin{pmatrix} \cos\frac{\alpha}{2} & \sin\frac{\alpha}{2} \\ -\sin\frac{\alpha}{2} & \cos\frac{\alpha}{2} \end{pmatrix}. \quad (7)$$

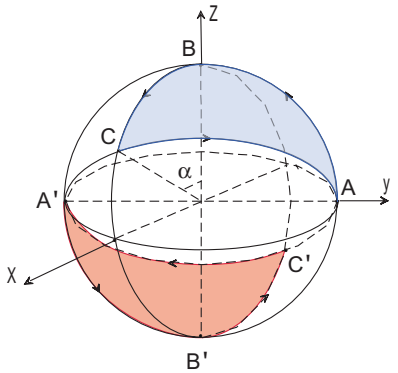

FIG. 2. (Color online) Cyclic trajectories used in the experiment. $|\psi_+\rangle$ is transported along the path A-B-C-A, and $|\psi_-\rangle$ is transported along the path A'-B'-C'-A'.

B. Controlled operations

We now apply this geometrical gate to controlled operations in a two-qubit system where qubit a is the control qubit, while qubit b undergoes the geometric circuit if qubit a is in state $|1\rangle$ but remains invariant if the control qubit is in state $|0\rangle$.

The Hamiltonian of the two-qubit system is (in angular frequency units)

$$H = \omega_a I_z^a + \omega_b I_z^b + 2\pi J I_z^a I_z^b. \tag{8}$$

For the subsystem of qubit b, we can write the reduced Hamiltonian

$$H_b = \omega_b I_z^b + 2\pi J m_z^a I_z^b = \left[\omega_b - 2\pi J\left(d^a - \frac{1}{2}\right)\right] I_z^b,$$

where m_z^a is the eigenvalue of I_z^a $\left(=\pm\frac{1}{2}\right)$ and d^a the corresponding computational value $(=0,1)$.

If we use a rotating frame with a frequency of $\omega_b' = \omega_b + \pi J$, the Hamiltonian vanishes for $d^a=0$, $H_b^{(0)}=0$, while it becomes $H_b^{(1)} = -2\pi J I_z^b$ for $d^a=1$.

This Hamiltonian generates controlled rotations around the z axis. To generate the trajectories of Fig. 2, we rotate the rotation axis using radio-frequency pulses. To generate a $\frac{\pi}{2}$ rotation around the x axis, e.g., we use the sequence

$$R_y^b\left(\frac{\pi}{2}\right) \to \frac{1}{4J} \to R_y^b\left(-\frac{\pi}{2}\right),$$

where the notation for the rotations is R_{axis}^{qubit} (angle), and $\frac{1}{4J}$ stands for free evolution under the control Hamiltonian for the duration $\tau = \frac{1}{4J}$. The circuit of Fig. 2 is thus generated by the sequence

$$R_y^b\left(\frac{\pi}{2}\right) \to \frac{1}{4J} \to R_y^b\left(-\frac{\pi}{2}\right) \to R_x^b\left(-\frac{\pi}{2}\right) \to \left(\frac{\alpha}{2\pi J}\right) \to R_x^b\left(\frac{\pi}{2}\right) \to R_y^b\left(-\alpha - \frac{\pi}{2}\right) \to \frac{1}{4J} \to R_y^b\left(\alpha + \frac{\pi}{2}\right). \tag{9}$$

This represents the first gate operation of Fig. 1. For the second operation, we have to reverse the roles of control and target qubit and apply the following sequence to qubit a:

$$R_y^a\left(\frac{\pi}{2}\right) \to \frac{1}{4J} \to R_y^a\left(-\frac{\pi}{2}\right) \to R_x^a\left(\frac{\pi}{2}\right) \to \frac{1}{2J} \to R_x^a\left(-\frac{\pi}{2}\right) \to R_y^a\left(\frac{\pi}{2}\right) \to \frac{1}{4J} \to R_y^a\left(-\frac{\pi}{2}\right), \tag{10}$$

now setting the rf frequency to $\omega_a + \pi J$.

IV. NUCLEAR MAGNETIC RESONANCE IMPLEMENTATION

For the experimental implementation, we used the two nuclear spins of ^{13}C-labeled chloroform as qubits. The system Hamiltonian corresponds to Eq. (8) with a spin-spin coupling constant $J=214.5$ Hz. Experiments were performed at room temperature on a Bruker AV-400 spectrometer.

The system was first prepared in a pseudopure state $|00\rangle$ using the method of spatial averaging [18] with the pulse sequence

$$R_x^b(\pi/3) \to G_z \to R_x^b(\pi/4) \to \frac{1}{2J} \to R_y^b(\pi/4) \to G_z, \tag{11}$$

which is read from left to right (as the following sequences). The rotations R_{axis}^{spins} (angle) are implemented by radio-frequency pulses. G_z is a pulsed-field gradient, which destroys all coherences (x and y magnetizations) and retains longitudinal magnetization (z magnetization component) only. $\frac{1}{2J}$ represents a free precession period of the specified duration under the coupling Hamiltonian (no resonance offsets).

From the state $|00\rangle$, we prepared the initial state $\frac{1}{\sqrt{2}}(|0\rangle + e^{i\varphi}|1\rangle)\otimes|0\rangle$ by rotating qubit a (the ^{13}C nuclear spin) into the xy plane. Experiments were done for $\varphi = \frac{n\pi}{2}$ $(n=0,1,2,3)$. For each value of φ, we performed the cloning operation, using the geometric gate operations (9) and (10) for different asymmetry parameters α.

To experimentally determine the fidelities (6), we need the density operators of the initial state of qubit a and the final states of both qubits. For this purpose, we parametrize the density operators as

$$\rho = \frac{1}{2}(1 + \vec{r}\cdot\vec{I}),$$

where $\vec{r}=(x,y,z)$ is a Bloch vector. The fidelities (6) are then

$$F_i = \mathrm{Tr}(\rho_0\rho_i) = \frac{1}{2}[1 + (\vec{r}_0\cdot\vec{r}_i)] \quad (i=a,b).$$

For the initial state $\psi = \frac{1}{\sqrt{2}}(|0\rangle + e^{i\varphi}|1\rangle)$, we have $\vec{r}_0 = (\cos\varphi, \sin\varphi, 0)$ and the fidelities become

$$F_i = \frac{1}{2}(1 + \cos\varphi x_i + \sin\varphi y_i). \tag{12}$$

The transverse components x_i, y_i can be measured as the transverse magnetization components of the free induction

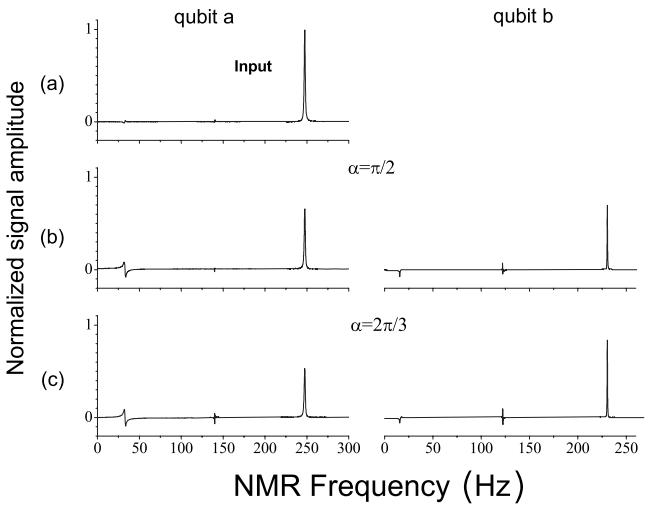

FIG. 3. Experimentally observed NMR spectra of ^{13}C chloroform before and after a quantum cloning operation. The original state was an equal-weight superposition with equal phases ($\varphi=0$), shown in the top row. The middle row shows the resulting spectra for a symmetric cloning operation ($\alpha=\pi/2$), and the bottom row shows the result of an asymmetric cloning operation ($\alpha=2\pi/3$). The left-hand column holds the input qubit and the right-hand column shows the copy qubit.

decay. To perform the trace over the other spin, we can either apply a decoupling field to the other spin or integrate over the two lines in the spectrum. For the present experiment, we chose the second possibility.

V. EXPERIMENTAL RESULTS

Figure 3 shows a typical example of a cloning operation. The input qubit (qubit a) was initialized into a pseudopure state $\frac{1}{\sqrt{2}}(|0\rangle+|1\rangle)$, as described in Sec. IV, using the phase angle $\varphi=0$, and the target qubit was set to $|0\rangle$. This state corresponds to transverse magnetization of spin a and is therefore directly observable in the NMR spectrometer. The upper row of Fig. 3 shows the Fourier transform of the measured free induction decay (FID) of the ^{13}C signal. Only one of the two resonance lines is observable, indicating that the target qubit is in the state $|0\rangle$.

The middle row of Fig. 3 shows the corresponding spectra after a symmetrical cloning operation, with the propagator of Eq. (7),

$$U\left(\alpha=\frac{\pi}{2}\right)=\frac{1}{\sqrt{2}}\begin{pmatrix}1 & -1\\ 1 & 1\end{pmatrix}.$$

Integrating the signal for each spin species, we find for the x components $x_a=0.667$ and $x_b=0.682$, in good agreement with the theoretical values of $x_a=x_b=1/\sqrt{2}$. The corresponding fidelities are $F_a=0.834$ and $F_b=0.841$ (theoretical values: 0.854).

The bottom row shows the same result for an asymmetric cloning operation. Here, the rotation angle α was set to $2\pi/3$. As a result, the target qubit has the higher fidelity: $F_a=0.758$, $F_b=0.920$, again in good agreement with the theoretical values of 0.750 and 0.933.

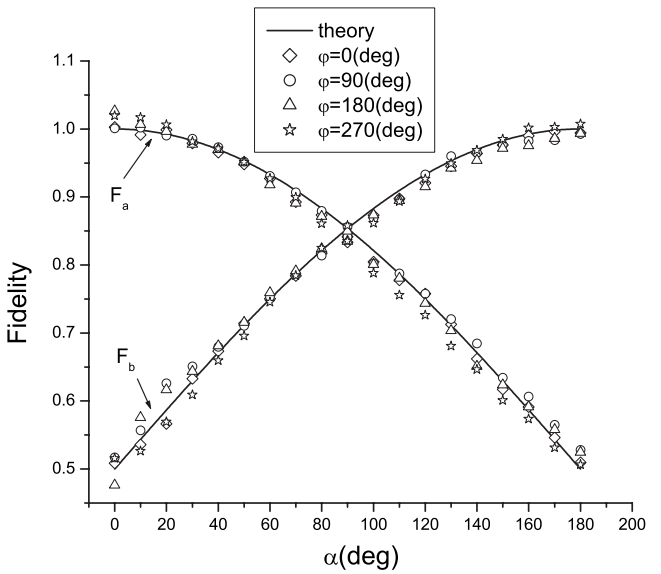

FIG. 4. Experimental fidelities versus the different parameter α of the asymmetric cloning machine. The theoretical values of fidelities are plotted as solid lines and the different symbols are corresponding to the experimental fidelities of two qubits with different angles φ of the initial state $|\psi\rangle_{ini}$.

Figure 4 shows a more systematic check of the effect of the rotation angle on the two fidelities. We compare the fidelities of both qubits with the theoretical value as a function of the asymmetry parameter α. The theoretical curve is independent of the phase of the initial state. Experimental data were measured for four different initial phases φ as a function of the rotation angle α. All four data sets are in good agreement with the expectation. The experimental errors ($\leqslant 0.031$), which are of the order of the size of the symbols, are mostly due to errors in the rotation angles of the radio-

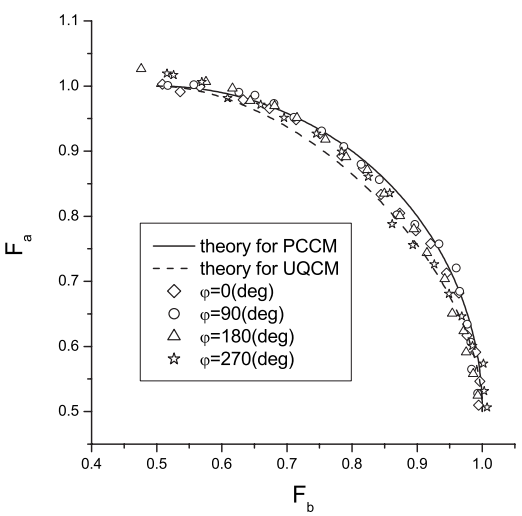

FIG. 5. Trade-off diagrams in the asymmetric cloning machine, respectively, for different phase angles φ of the initial state $|\psi\rangle_{ini}$. The full line shows the theoretical expectation for phase-covariant cloning, while the dashed line represents the limiting value for a universal cloning machine. The different symbols refer to experimental data points for different initial conditions.

frequency pulses, which arise from the inhomogeneity of the radio-frequency field. For vanishing rotation, the input qubit is not disturbed ($F_a \approx 1$), while the target qubit bears no information ($F_b \approx 0.5$). For a π rotation, the roles of original and target qubit are reversed, and at $\alpha = \pi/2$, both qubits share the information equally.

This apparent complementarity of the two fidelities can be quantified. According to Eqs. (5), the points (F_a, F_b) are located on a quarter circle whose origin is at (0.5,0.5) and whose radius is 0.5. Figure 5 verifies this relation. Here, the experimental fidelities are plotted against each other for different rotation angles α and different initial phases φ, represented by the different symbols. All experimental points are close to the circle representing the theoretical expectation [34]. The dashed curve in Fig. 5 represents the theoretical prediction for a universal cloning machine [15]. Evidently, the theoretical curve for phase-covariant cloning as well as the experimental data are outside of this range, except for angles close to 0 or π, where the information is located on a single qubit.

VI. CONCLUSION

In summary, we have experimentally realized an optimal asymmetric $1 \rightarrow 2$ phase-covariant cloning machine. As a function of a continuous-angle variable in the cloning operation, the phase information of the input state is transferred to the two output states such that either the original qubit is only slightly disturbed ($\alpha \rightarrow 0$) or that most of the phase information is transferred to the second qubit ($\alpha \rightarrow \pi$). The case of symmetric cloning is recovered for $\alpha = \frac{\pi}{2}$.

In the case of quantum cryptography, this tradeoff determines how much information the eavesdropper can gain for a given disturbance of the transmitted information. The fidelities found for this phase-covariant cloning were higher than the upper bound for universal cloning.

The cloning was implemented experimentally on an NMR quantum information processor. For the cloning operations, we used cyclic rotations of the qubits in such a way that the system acquired a geometrical phase. This procedure has been proposed for shielding the gate operation from such perturbations that leave the area of the quantum-mechanical trajectory invariant and thereby improve the overall fidelity.

ACKNOWLEDGMENTS

We thank Professor Z. D. Wang and Dr. Q. Chen for helpful discussions. This work is supported by the NNSF of China, the CAS, and the National Fundamental Research Program. It was also supported by Marie Curie Action program of the European Union.

[1] D. Dieks, Phys. Lett. **92A**, 271 (1982).
[2] W. K. Wootters and W. H. Zurek, Nature (London) **299**, 802 (1982).
[3] V. Scarani, S. Iblisdir, N. Gisin, and A. Acin, Rev. Mod. Phys. **77**, 1225 (2005).
[4] V. Bužek and M. Hillery, Phys. Rev. A **54**, 1844 (1996).
[5] N. J. Cerf, Acta Phys. Slov. **48**, 115 (1998).
[6] N. J. Cerf, Phys. Rev. Lett. **84**, 4497 (2000).
[7] N. J. Cerf, J. Mod. Opt. **47**, 187 (2000).
[8] C. S. Niu and R. B. Griffiths, Phys. Rev. A **58**, 4377 (1998).
[9] S. Iblisdir, A. Acin, and N. J. Cerf, R. Filip, J. Fiurasek, and N. Gisin, Phys. Rev. A **72**, 042328 (2005).
[10] S. L. Braunstein, V. Bužek, and M. Hillery, Phys. Rev. A **63**, 052313 (2001).
[11] A. E. Rastegin, Phys. Rev. A **66**, 042304 (2002).
[12] R. Filip, Phys. Rev. A **69**, 032309 (2004).
[13] R. Filip, Phys. Rev. A **69**, 052301 (2004).
[14] Z. Zhao, A. N. Zhang, and X. Q. Zhou Y. A. Chen, C. Y. Lu, A. Karlsson, and J. W. Par, Phys. Rev. Lett. **95**, 030502 (2005).
[15] D. Bruss, M. Cinchetti, G. M. D'Ariano, and C. Macchiavello, Phys. Rev. A **62**, 012302 (2000).
[16] W. H. Zhang, L. B. Yu, and L. Ye, Phys. Lett. A **356**, 195 (2006).
[17] J. Du, T. Durt, and P. Zou *et al.*, Phys. Rev. Lett. **94**, 040505 (2005).
[18] D. G. Cory, M. D. Price, and T. F. Havel, Physica D **120**, 82 (1998).
[19] S. L. Zhu and P. Zanardi, Phys. Rev. A **72**, 020301(R) (2005).
[20] M. V. Berry, Proc. R. Soc. London, Ser. A **392**, 45 (1984).
[21] Y. Aharonov and J. Anandan, Phys. Rev. Lett. **58**, 1593 (1987).
[22] S. L. Zhu, Z. D. Wang and Y. D. Zhang, Phys. Rev. B **61**, 1142 (2000).
[23] S. L. Zhu and Z. D. Wang, Phys. Rev. Lett. **85**, 1076 (2000).
[24] P. Zanardi and M. Rasetti, Phys. Lett. A **264**, 94 (1999).
[25] G. Falci, R. Fazio, and G. M. Palma *et al.*, Nature (London) **407**, 355 (2000).
[26] L. M. Duan, J. I. Cirac, and P. Zoller, Science **292**, 1695 (2001).
[27] J. A. Jones, V. Vedral, A. Ekert, and G. Castagnoli, Nature (London) **403**, 869 (2000).
[28] Xiang-Bin Wang and M. Keiji, Phys. Rev. Lett. **87**, 097901 (2001).
[29] S. L. Zhu and Z. D. Wang, Phys. Rev. Lett. **89**, 097902 (2002).
[30] S. L. Zhu and Z. D. Wang, Phys. Rev. A **67**, 022319 (2003).
[31] S. L. Zhu and Z. D. Wang, Phys. Rev. A **66**, 042322 (2002).
[32] X. D. Zhang, S. L. Zhu, L. Hu, and Z. D. Wang, Phys. Rev. A **71**, 014302 (2005).
[33] J. F. Du, P. Zou, and Z. D. Wang, Phys. Rev. A **74**, 020302(R) (2006).
[34] G. M. D'Ariano and C. Macchiavello, Phys. Rev. A **67**, 042306 (2003).